

Transposed Paternò–Büchi Reaction

Elango Kumarasamy,[†] Ramya Raghunathan,[†] Sunil Kumar Kandappa,[†] A. Sreenithya,[‡] Steffen Jockusch,^{*,§} Raghavan B Sunoj,^{*,‡} and J. Sivaguru^{*,†}

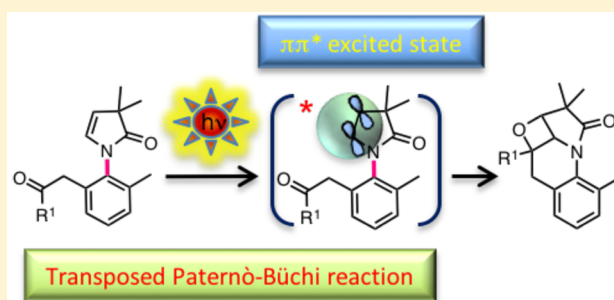
[†]Department of Chemistry and Biochemistry, North Dakota State University, Fargo, North Dakota 58108, United States

[‡]Department of Chemistry, Indian Institute of Technology Bombay, Powai, Mumbai, 400076. India

[§]Department of Chemistry, Columbia University, New York, New York 10027, United States

Supporting Information

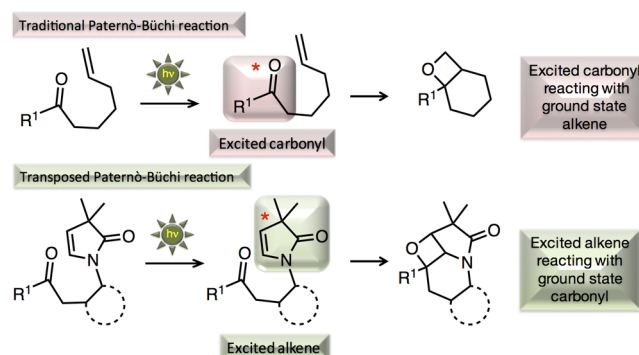
ABSTRACT: A complementary strategy of utilizing $\pi\pi^*$ excited state of alkene instead of $n\pi^*$ excited state of the carbonyl chromophore in a “transposed Paternò–Büchi” reaction is evaluated with atropisomeric enamides as the model system. Based on photophysical investigations, the nature of excited states and the reactive pathway was deciphered leading to atropselective reaction. This new concept of switching of excited-state configuration should pave the way to control the stereochemical course of photoreaction due to the orbital approaches required for photochemical reactivity.



INTRODUCTION

Synthetic methodologies that enable us to access diverse and complex structural motifs with precise control over stereochemistry are highly pursued in the field of organic chemistry and drug discovery.¹ In this regard, photochemical transformations hold great promise as they enable us to build rapid complexity with relative ease, using environmentally friendly methods.² While it is very alluring in terms of its synthetic potency, its applicability is often hindered by our inability to control the short-lived excited states to steer it into the desired chemical pathway. This challenge often limits its wide scope in synthetic organic chemistry especially in stereoselective photo-transformations.³ To address this bottleneck, several avenues were evaluated, including confined environments, crystalline media, and templated hosts to name a few. All these strategies restrict the excited-state reactants rigidly in a reaction-ready state for an efficient photoinduced process.⁴ While the success of this approach had significant impact on the outcome of the stereoselectivity in photoproduct(s), the idea could not be extended with the same level of success to the reactions that happen in solution, where such steric or conformational bias are either absent or inefficient. To find an alternative solution to this challenge, research in our group is geared toward the development of atropselective reactions where the selectivity is dictated by restricted bond rotation(s) in the reactive chromophores.⁵ We were successful in employing this strategy for achieving high selectivity in the photoproducts for various light induced transformations.⁶ To expand on the potential of our methodology, we investigated the synthetically useful Paternò–Büchi reaction, where the oxetane product is typically formed by an addition of excited carbonyl chromophore to a ground state alkene (Scheme 1; top).⁷

Scheme 1. Paternò–Büchi Reactions^{4a}



^aTraditional, where carbonyl group is excited for photoreactions; transposed, where alkene motif is excited for oxetane formation.

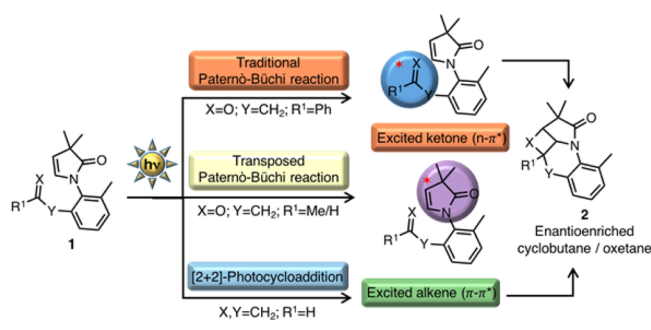
However, in our investigation, we envisioned switching the reactivity of excited states involved in the Paternò–Büchi reaction where the alkene chromophore is photoexcited that further reacts with a ground state carbonyl group (Scheme 1; bottom). We term this change in excited state as “transposed Paternò–Büchi” reaction where alkene’s $\pi\pi^*$ excited state initiates the reaction resulting in the oxetane product rather than traditional $n\pi^*$ excited state of the carbonyl group. While conceptually it is simple to discern either of the excited states lead to the same oxetane product, to the best of our knowledge, experimentally no such observation has been documented in the literature so far.

Received: June 17, 2016

Published: December 13, 2016

Fundamentally, we felt this investigation is very compelling because the change in the nature of excited state will have a profound consequence in the orbitals that initiates the photoreaction leading to the oxetane product. For example, an excited carbonyl typically triggers a reaction from an $n\pi^*$ excited state, while an excited alkene could trigger the reaction from a $\pi\pi^*$ excited state.⁸ In addition, our approach provides a complementary strategy to existing reports that not only allow us to access chirally enriched cyclobutane or oxetane from a single building block but also circumvents side reactions that are associated with excited-state chemistry of carbonyl chromophores such as hydrogen abstraction, disproportionation, and self-coupling to form pinacol type products.^{7a,9} To explore the concept of excited-state switching, we selected a model system based on cyclic enamide **1** (Scheme 2).¹⁰ By

Scheme 2. Manipulating Excited-State Reactivity of Atropisomeric Enamides



suitably engineering the tether and controlling the reaction conditions, we anticipated altering the excited state leading to transposed Paternò-Büchi reaction. For example, enamides with the alkene (Scheme 2; bottom) or aldehyde/alkyl ketone (Scheme 2; middle) could enable us to initiate photochemical reactivity from an enamide chromophore. However, an aromatic ketone will likely react from excited-state carbonyl chromophore leading to traditional Paternò-Büchi reaction (Scheme 2; top). There are few reports in the literature that describe the intermolecular Paternò-Büchi reaction of dihydro-2-pyridones, which is a six-membered enamide.¹¹ However, in these instances dihydro-2-pyridones are only used as a ground-state partner for the excited-state carbonyl group (traditional Paternò-Büchi reaction), and photoreactions originating from the excited state of the enamide remain unexplored.

RESULTS AND DISCUSSION

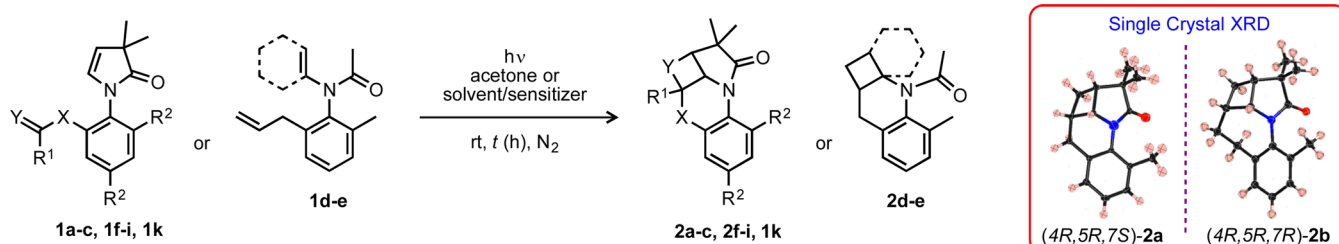
To carry out systematic investigations, we synthesized various atropisomeric enamide derivatives and evaluated their racemization barrier and photochemical reactivity (Tables 1 and 2).¹² The five-membered cyclic enamides **1a–c** were prepared with pendant allyl, butenyl, and *O*-allyl tethers, respectively. To gain more insights into the structural attributes of the enamide chromophore, we synthesized acyclic enamides **1d,e**. The understanding of the excited state reactivity of **1a–e** (*vide infra*) led us to design cyclic enamides tethered to phenyl ketone **1f**, aldehyde **1g** and **1i**, and methyl ketone **1h**. The cyclic enamides **1a,b** were easily synthesized as racemates from the corresponding aniline and anhydride derivatives (Scheme 3), and the synthesis of **1c** is detailed in the Supporting Information. Heating a neat mixture of aniline **3** and anhydride **4** to 190 °C resulted in the condensation reaction yielding

Table 1. Racemization Rate Constant (k_{rac}), Half-Life ($\tau_{1/2}$), and Activation Free Energy ($\Delta G_{\text{rac}}^\ddagger$) for Optically Pure Enamides^a

entry	compd	k_{rac} (s ⁻¹)	$\tau_{1/2}$ (h)	$\Delta G_{\text{rac}}^\ddagger$ (kcal·mol ⁻¹)
1	1a	4.1×10^{-5}	4.7	27.5
2	1b	2.0×10^{-5}	9.6	28.0
3	1c ^b	2.6×10^{-4}	0.7	22.2
4	1e	1.1×10^{-5}	17.8	28.4
5	1f	2.1×10^{-4}	0.9	26.3

^aThe racemization kinetics was performed on optically pure isomers at 75 °C in 2-propanol (IPA). ^bFor **1c**, the racemization was done in hexanes–IPA mixture at 23 °C. The racemization values carry an error of $\pm 5\%$. Refer to Supporting Information for more information.

corresponding imide derivatives **5**. The imide was reduced to aminol using DIBAL at –78 °C followed by mesylation and base-induced elimination to furnish atropisomeric enamides **1** (Scheme 3, top). Carbonyl analogues **1f–i** were also synthesized in the same synthetic sequence but with protected alcohol **3f–i**, which at later stages was deprotected and oxidized to reveal the carbonyl functionality.¹³ The presence of gem dimethyl group in the newly synthesized enamides is crucial to avoid decomposition when stored over a period of time. This is in line with the reported observations that some of the *N*-substituted pyrrol-2-ones are unstable and undergo isomerization/dimerization reactions.¹⁴ The acyclic enamides **1d,e** were obtained from corresponding anilines and carbonyl derivatives in a two-step sequence, *viz.*, formation of imine followed by acylation in the presence of a base (Scheme 3-bottom). All newly synthesized enamides were characterized by ¹H and ¹³C NMR spectroscopy, HRMS, optical rotations, and HPLC analyses. The enantiomerically pure isomers required for the racemization studies and atropselective photoreactions were easily secured by separation through a chiral stationary phase using HPLC in very high enantiomeric purity (>98%).¹² The axial chirality of the enamides solely rests in the *N*–C_{Aryl} pivotal bond, and the energy barrier to rotation is dictated by the steric bulk around the *N*–C_{Aryl} chiral axis. The racemization barrier for enamides were found to be between 26 and 28 kcal/mol at 75 °C in 2-propanol except for **1c** (Table 1). In **1c**, where the methylene group of the alkenyl tether was substituted for oxygen, the energy barrier to rotation was significantly reduced (Table 1; entry 3), leading to racemization even at ambient temperature (23 °C). For atropselective phototransformation, having a higher energy barrier is critical as it translates to efficient chirality transfer (axial to point chirality transfer). In contrast, a low *N*–C_{Aryl} energy barrier for rotation will lead to inefficient chirality transfer and poor selectivity in the photoproducts. Photoreactions were carried out with a 450W medium pressure Hg lamp placed inside a water-cooled jacket with a Pyrex cutoff filter under constant flow of nitrogen. The reaction proceeded smoothly under sensitized irradiation conditions in either acetone (as both solvent and sensitizer) or a solution of acetonitrile with triplet sensitizers such as xanthone or acetophenone. The direct irradiation of enamides did not yield the desired product, and in most cases, the starting material was recovered with appreciable decomposition. Under sensitized irradiation conditions, the conversion depended on the type of sensitizers employed. For example, 30 min irradiation of **1a** in the presence of acetone (both solvent and sensitizer), xanthone, and acetophenone resulted in >98%, ~84%, and ~38% conversion, respectively (Table 2, entry 1).

Table 2. Atropselective [2 + 2]-Photocycloaddition of Enamides 1a–i^a

Entry	Substrate	Solv/Sens.	t (h)	Product	[%] Yield, [%] ee [%] Convn. (MB)	Entry	Substrate	Solv/Sens.	t (h)	Product	[%] Yield, [%] ee [%] Convn. (MB)
1		acetone	0.5		Yield = 85% (-)-(4S,5S,7R)-2a > 98% ee (+)-(4R,5R,7S)-2a > 98% ee	5		acetone	6	- ^c	-
		MeCN/xanthone	0.5	2a	84 (89) ^b	6		acetone	8		94 (82) ^{b,d}
		MeCN/acetophenone	0.5	2a	38 (88) ^b			THF	3		Yield = 75% ^e
2		acetone	1.3		Yield = 77% (-)-(4S,5S,7S)-2b > 96% ee (+)-(4R,5R,7R)-2b > 96% ee			MeCN/xanthone	12		62 ^{d,e}
		MeCN/xanthone	1.3	2b	84 (94) ^b	7		acetone	1		Yield = 70%
		MeCN/acetophenone	1.3	2b	20 (92) ^b	8		acetone	2.5		78
3		acetone	1.3		Yield = 72% (A)-2c < 20% ee (B)-2c < 20% ee			MeCN	2.5		< 7 ^b
						8		MeCN/xanthone	2		Yield = 73% ^f
4		acetone	6	- ^c	-	9		MeCN/xanthone	0.5		Yield = 52%
											72% ee ^g 88% ee ^g

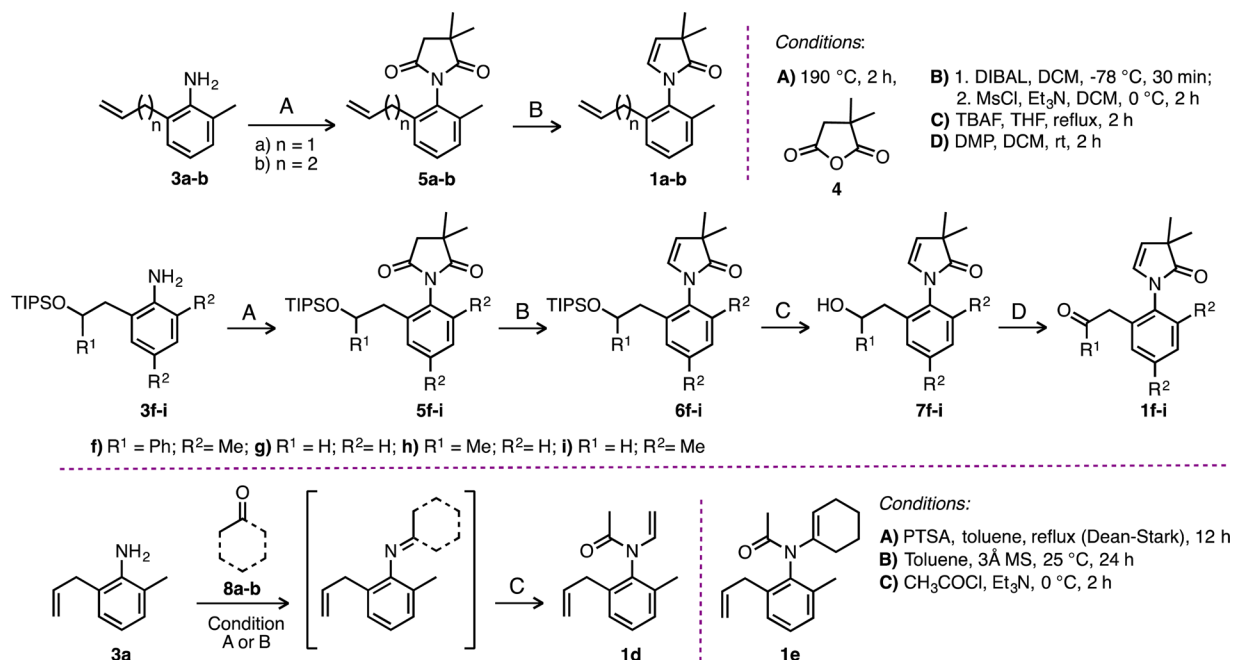
^aPhotoreactions were performed at room temperature using 450 W medium pressure mercury lamp. Acetone as solvent and sensitizer or MeCN/30 mol % sensitizer. (+) and (–) represent the sign of optical rotation (MeOH at 25 °C). A and B refer to the elution order for a given pair of enantiomers in the HPLC. Reported values are an average of 3 runs with $\pm 3\%$ error. The yields reported are isolated yield after column chromatography. The numbering positions are labeled as a guide to denote stereochemistry. The ee values were determined by HPLC on a chiral stationary phase. Absolute configuration determined by single-crystal XRD using Flack parameters. ^bConversion (%Conv.) and mass balance (MB, in parentheses) are based on ¹H NMR using triphenylmethane as internal standard. For **1b**, ~5% of uncharacterized enantiomeric impurity was observed. ^cNo photoreaction was observed. ^dThe reaction was performed at –30 °C to avoid the formation of uncharacterized side product and to improve the ee values (at 25 °C, an ee value of 72% was observed). ^eA Rayonet reactor with lamps of approximately 350 nm light output was used for irradiations. ^fThe yield is based on ¹H NMR spectroscopy. ^gThe optical purity of PkA and PkB of **1i** are 76 and 92%, respectively.

This observation is probably due to the triplet energy and differential absorption coefficient of the sensitizers, i.e., xanthone has a much larger absorption cross section in the near-UV compared to that of acetophenone and thus efficiently absorbs more photons leading to better sensitization of the reaction. After the reaction, the solvent was evaporated under reduced pressure and the crude product was purified by

chromatography and analyzed by ¹H and ¹³C NMR spectroscopy. The structure elucidation of the photoproduct was done by single-crystal XRD, and the absolute configuration was established by Flack parameters (Table 2).

Inspection of Table 2 clearly shows distinctive behavior in the photoreaction of atropisomeric enamides **1a–i**. Five-membered cyclic enamides **1a–c** reacted in a facile manner

Scheme 3. Synthesis of Cyclic (Top) and Acyclic (Bottom) Enamides

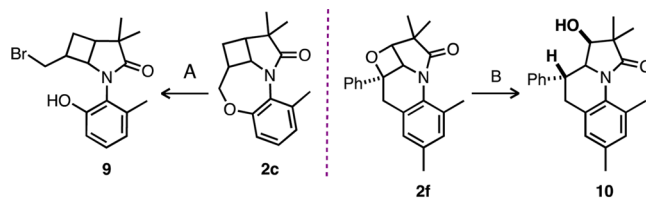


leading to corresponding cyclobutane products **2a–c** with good isolated yields (Table 2; entries 1–3). However, the enantiomeric excess (ee) in the product depended on the type of alkenyl chain employed. For example, allyl and butenyl derivatives **1a,b** resulted in very high ee in the product (Table 2; entry 1 and 2). But in the case of enamide **1c**, where the methylene group of the butenyl tether was replaced with oxygen, the ee of the reaction drastically reduced (ee < 20%; Table 2, entry 3). The low atropselectivity has its origin in the fast racemization ($\tau_{1/2} = 0.7$ h at 23 °C; Table 1, entry 3) under the reaction conditions. The racemization was competing with the photoreaction leading to diminished ee values in the product. Examination of the photoproducts from enamides **1a–c** revealed that in all the cases only straight photocycloaddition product was observed and cross photoproduct(s) were not noticed.¹⁵

Acyclic enamides **1d,e** failed to undergo the desired photoreaction under both sensitized and direct irradiation conditions. This observation was surprising to us, as the basic chromophore was still present in the acyclic enamides. The absence of cyclic chromophore can affect the photoreactivity of enamides in many ways. First, the orientation of the enamide double bond could be unfavorable that inhibits the approach of the reacting ground state alkene tether (Figure S4). Second, the triplet energy of the acyclic enamides becomes higher than that of the cyclic enamides, which makes the sensitization process inefficient. These assertions were supported by photophysical studies carried out on acyclic enamide **1e** in the presence of the sensitizer (*vide infra*). Finally, even if the energy is transferred during sensitization, the triplet excited-state lifetime of a nonrigid chromophore such as acyclic enamide can be drastically reduced through vibrational relaxation.¹⁶

The observations on excited-state reactivity and the estimation of triplet energy (*vide infra*) of enamides **1a–e** led us to design substrates for traditional (**1f**) and transposed Paternò–Büchi reaction (**1g–i**). Direct excitation of the benzoyl chromophore in **1f** results in reactive $n\pi^*$ triplet excited state through efficient spin–orbit coupling (in excited

carbonyl species) leading to traditional Paternò–Büchi reaction.^{7d–f} Comparison of substrates **1a–e** (that feature a $\pi\pi^*$ triplet excited state on the enamide) and **1f** presented an interesting question. Can we design substrates where one can access the $\pi\pi^*$ triplet excited state irrespective of having a carbonyl functionality? To explore this possibility, we investigated substrates **1g–i** as one can expect the lowest $\pi\pi^*$ triplet excited state to be localized on the enamide chromophore that can be accessed by triplet energy transfer from an appropriate sensitizer leading to transposed Paternò–Büchi reaction. Under sensitized irradiation conditions similar to those employed for **1a–c**, enamides **1f–i** smoothly underwent photocycloaddition to furnish corresponding oxetane photoproducts **2f–i**. Atropisomeric phenyl ketone derivative **1f** underwent atropselective reaction to furnish oxetane product **2f** in good ee (88% at -30 °C; Table 2; entry 6). The room-temperature reaction resulted in significant amount of uncharacterized side product and reduced ee values. Similarly, atropisomeric aldehyde derivative **1i** resulted in high ee values as well (Table 2; entry 9). Oxetane photoproducts **2c** and **2f** was ring-opened to reveal corresponding alcohol derivatives (Scheme 4). For example, the ether linkage in **2c** was efficiently cleaved using BBr₃ in DCM resulting in 71% of phenolic product **9**.^{6f} Similarly, the ether linkage in **2f** was

Scheme 4. Tether Cleavage of Oxetane and Cyclobutane Photoproducts **2f** and **2c**^a

^aA: BBr₃, DCM, 25 °C, 12 h (yield = 71%); B: Pd(OH)₂, MeOH, 25 °C, 2 h (yield = 93%).

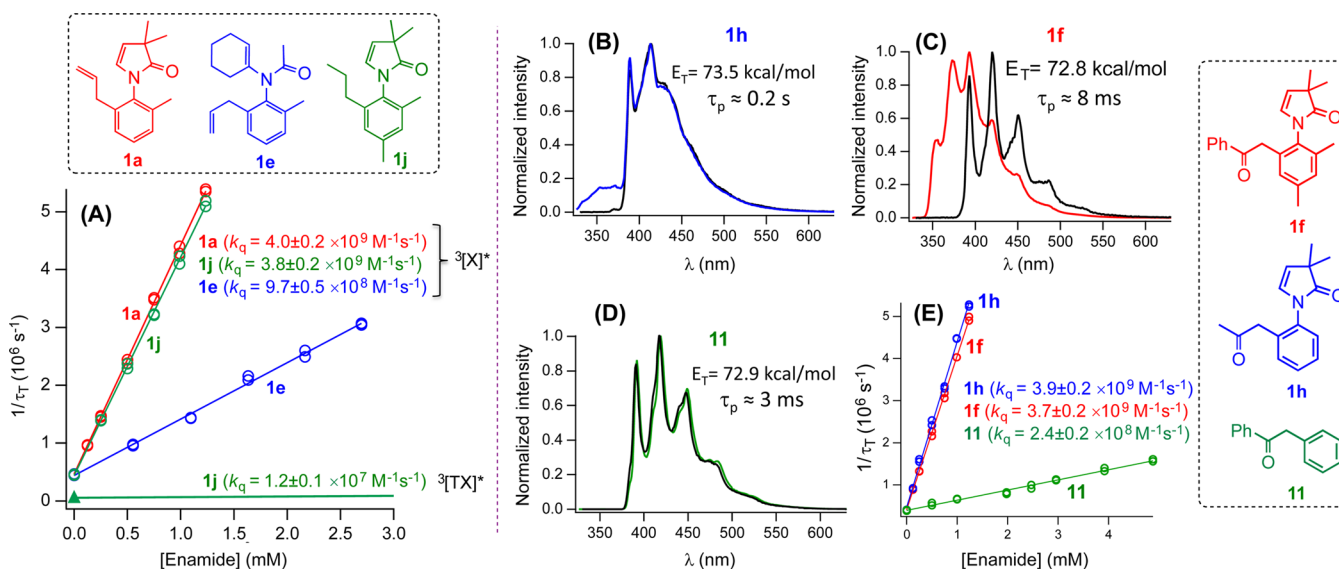


Figure 1. (A) Determination of the bimolecular rate constants of quenching of xanthone triplet $^3[X]^*$ with **1a**, **1e**, and **1j** and thioxanthone triplet $^3[TX]^*$ states with **1j** using laser flash photolysis ($\lambda_{\text{ex}} = 355 \text{ nm}$, 7 ns pulse width). Inverse triplet lifetime determined from triplet absorption decay traces monitored at 620 nm with varying concentration of enamides in argon saturated acetonitrile solutions. (B) Luminescence spectra of **1h** (blue: steady-state; black: time-resolved). (C) Luminescence spectra of **1f** (red: steady-state; black: time-resolved). (D) Luminescence spectra of **11** (green: steady-state; black: time-resolved) measured in ethanol glass at 77K. (E) Determination of the bimolecular quenching rate constants k_q of quenching of xanthone triplet states by **1h** (blue), **1f** (red), and **11** (green) using laser flash photolysis ($\lambda_{\text{ex}} = 355 \text{ nm}$, 7 ns pulse width). Inverse xanthone triplet lifetime determined from triplet absorption decay traces monitored at 620 nm vs varying concentration of **1h**, **1f**, and **11** in argon-saturated acetonitrile solutions.

cleaved using $\text{Pd}(\text{OH})_2$ in methanol to yield corresponding alcohol **10** in good yield (93%).^{11b}

Carbonyl derivatives **1f–i** employed in the reaction are distinct in their photochemistry. Direct irradiation of enamides **1g** and **1i** with an aldehyde tether did not result in the oxetane product (similar to the reactivity of enamides **1a–c**). However, methyl ketone derivative **1h** showed low reactivity under direct irradiation. For example, direct irradiation of **1h** in MeCN at room temperature for 2.5 h resulted in $\sim 7\%$ of **2h**, while the sensitized irradiation resulted in complete conversion within 2.5 h. In the case of phenyl ketone **1f**, the conversion under direct irradiation was comparable to that of the sensitized irradiation. For instance, conversion of **1f** under sensitized (acetone) and direct irradiation (THF) at room temperature for 3 h was $>98\%$ and $>94\%$, respectively. The differences in conversions observed between **1f** and **1h** provides insight into the extinction coefficient of the particular carbonyl chromophore involved. In the case of **1h**, the methyl ketone chromophore (analogues to acetone) has the ability to absorb the photons albeit with poor efficiency that is reflected in very low conversion during direct irradiation. However, when phenyl ketone derivative **1f** was employed (analogous to acetophenone), the absorption of photons increased considerably that resulted in conversion comparable to sensitized irradiation.

The analysis of results from **1f–i** reveals that oxetanes **2f–i** are formed from two different excited states depending on the substrate that is undergoing the transformation and the type of irradiation. Under direct irradiation, **1f** undergoes a traditional Paternò–Büchi reaction in which the phenyl ketone is excited ($n\pi^*$) that reacts with ground-state enamide alkene, whereas in the presence of a sensitizer, the enamide part of the molecule is excited ($\pi\pi^*$) via triplet energy transfer. This conclusion was arrived from photophysical studies carried out on **1f** and 2-phenylacetophenone **11** (*vide infra*). Enamides **1g–i** undergo a transposed Paternò–Büchi reaction in which the enamide is

excited by sensitization (while no reaction was observed under direct irradiation). To substantiate our conjecture that enamide excited state is involved in the formation of oxetane product (rather than carbonyl excited state), we carried out detailed photophysical studies on enamides and compared that to our experimental results.

Photophysical studies were carried out on two sets of enamides. In the first set, we utilized cyclic enamides **1a**, nonreactive acyclic enamide **1e**, and enamide **1j** that lacked the double bond for photocycloaddition reaction (Figure 1A). Enamide **1j** was specifically chosen to prevent any photochemical reaction and to characterize the excited state of the enamide chromophore. In the second set, enamides with the carbonyl chromophore were selected, *viz.*, **1h** (enamide with methyl ketone), **1f** (enamide with phenyl ketone), and **11** phenyl ketone derivative that lacked the enamide chromophore (Figure 1B–E). Enamides **1a**, **1e**, and **1j** showed no observable luminescence at room temperature or in frozen matrix at 77 K. As the reaction was carried out under sensitized conditions with xanthone as the triplet sensitizer, we used laser flash photolysis to understand the excited-state reactivity of enamides in the presence of xanthone (Figure 1A). Using laser flash photolysis ($\lambda_{\text{ex}} = 355 \text{ nm}$, 7 ns pulse width),¹⁷ we determined the bimolecular quenching rate constants (k_q) of xanthone triplet states by **1a** (red), **1j** (green), and **1e** (blue) in argon-saturated acetonitrile solutions (Figure 1A). The triplet states of xanthone $^3[X]^*$ were efficiently quenched by enamides with very high rate constants. For example, the quenching rate constants (k_q) of **1a** and **1j** were 4.0×10^9 and $3.8 \times 10^9 \text{ M}^{-1} \text{ s}^{-1}$ respectively. The quenching rate constant (k_q) of **1e** (nonreactive enamide) was an order of magnitude lower at $9.7 \times 10^8 \text{ M}^{-1} \text{ s}^{-1}$.

Experimentally identical quenching rate constants for **1a** and **1j** indicate that the excited state resides in the enamide functionality. Using thioxanthone as sensitizer, which has a

lower triplet energy ($E_T = 63$ kcal/mol) than xanthone ($E_T = 74$ kcal/mol), a more than 2 orders of magnitude lower quenching rate constant for **1j** was observed (1.2×10^7 M⁻¹ s⁻¹; Figure 1A). This indicates that the triplet energy of enamides is significantly higher than 63 kcal/mol but lower than 74 kcal/mol. The low thioxanthone triplet quenching rate constant is consistent with the absence of photoreaction in **1a** when thioxanthone is used as sensitizer. In order to unequivocally establish the excited state that likely resides on the enamide chromophore, quenching studies of xanthone triplets were carried out with **5a** that lacked the enamide double bond. The quenching rate constant for **5a** was an order lower than that of parent enamide **1a** ($k_q = 3.9 \times 10^7$ M⁻¹ s⁻¹; Figure S7). This shows that the quenching of the xanthone triplet by **1a** is kinetically controlled and that the triplet energy is transferred to the enamide chromophore with maximum rate constants for triplet energy transfer rather than to the alkene tether (as **5a** has a lower k_q).

We then turned our attention to evaluate enamides **1f** and **1h**, featuring a carbonyl tether, and 2-phenylacetophenone **11**. Substrate **11** was used as model benzoyl chromophore, which contains the carbonyl functionality, but not the enamide chromophore. Steady-state and time-resolved luminescence spectra were recorded in ethanol glass at 77 K (Figure 1B–D). Based on the time-resolved phosphorescence spectra, the triplet energies of **1h**, **1f**, and **11** were estimated to be 73.5, 72.8, and 72.9 kcal/mol, respectively. The phosphorescence of **1f** and **11** showed a lifetime of 8 and 3 ms, respectively, indicating that the lowest excited triplet features a $n\pi^*$ configuration. In contrast, enamide **1h** showed a phosphorescence lifetime of 0.2 s, indicating a $\pi\pi^*$ triplet state. This phosphorescence was assigned to the enamide chromophore in **1h**. The bimolecular quenching rate constants (k_q) were determined by quenching of xanthone triplet states by **1h** (blue), **1f** (red), and **11** (green) using laser flash photolysis ($\lambda_{ex} = 355$ nm, 7 ns pulse width; Figure 1E). The triplet state of the xanthone sensitizer was efficiently quenched by enamides with very high rate constants. For example, the quenching rate constants (k_q) of **1h** and **1f** were 3.9×10^9 and 3.7×10^9 M⁻¹ s⁻¹, respectively. However, the quenching rate constant (k_q) of **11** was an order of magnitude lower at 2.4×10^8 M⁻¹ s⁻¹ compared to **1f**. Similar quenching rate constants for the two sets of enamides, **1a/1j** and **1h/1f**, shows that the triplet excited state of the enamide is lower than that of xanthone (74 kcal/mol). This result clearly explains the efficiency of xanthone in sensitizing the reaction involving enamide excited state. This difference in the quenching rate constant between **11** and **1f** suggests that the energy transfer from xanthone triplets to the enamide chromophore might be more efficient in comparison to energy transfer to the carbonyl chromophore leading to transposed Paternò–Büchi reaction. An alternative scenario, where the energy transfer from enamide chromophore to phenyl ketone (intramolecular energy transfer) leads to traditional Paternò–Büchi reaction, can not be ruled out.¹⁸ This hypothesis is also supported by the fact that the **1f** and **11** have similar phosphorescence lifetimes at 77 K suggesting an $n\pi^*$ excited state. While under direct irradiation, **1f** results in $n\pi^*$ excited state leading to traditional Paternò–Büchi reaction, whereas sensitization of **1g–i** results in a $\pi\pi^*$ triplet excited state of the enamide moiety leading to a transposed Paternò–Büchi reaction.

To further establish the nature of orbital involved in the transposed Paternò–Büchi reaction, we performed detailed

computational studies. (See the Computational Methods section for more details.) The triplet vertical excitations have been calculated using the linear-response time-dependent density functional theory (TD-DFT) at the CAM-B3LYP/6-31+G* level of theory. While the computed vertical triplet transitions (Table S2) are slightly higher (by ~5 kcal/mol) than the triplet energies observed experimentally, the orbital ordering is expected to remain the same. For all chromophores, the HOMO was found to be located on the enamide double bond region of the molecule. In all cases, the lowest energy triplet excitation is of $\pi_{\text{enamide}} \rightarrow \pi^*$ character, which is in line with the experimental observations. In chromophores **1a–1e** that contain an external alkene tether, the excited state is found to involve the π^* molecular orbitals of the aryl as well as that on the cyclic enamide moiety. However, in **1g–1i**, the π^* is located on the carbonyl side chain. Two important orbital contours are provided as representative examples for **1b** and **1g** in Figure 2. It can be noticed that two of the lower energy

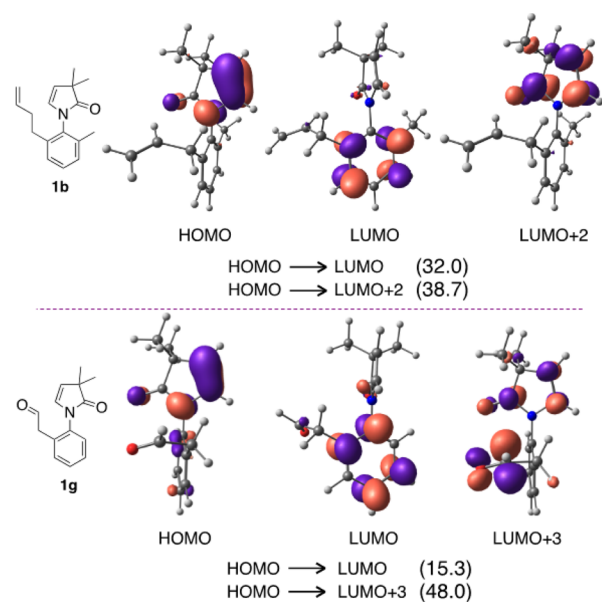


Figure 2. Frontier molecular orbitals involved in the $\pi_{\text{enamide}} \rightarrow \pi^*$ triplet excited state of **1b** and **1g** (generated using an isosurface value of 0.0622). The percentage of contribution of the major transitions is given in parentheses.

unoccupied orbitals, LUMO and LUMO+2 for **1b**, are the respective π^* molecular orbitals of the aryl and the cyclic enamide fragments. In the lowest triplet excited state, the contribution of LUMO and LUMO+2 is about 70.7% in **1b**. In the calculations, a hypothetical vertical excitation ($S_0 \rightarrow T_1$) in the case of **1g** was found to be from the HOMO (π_{enamide}) to LUMO+3 ($\pi^*_{\text{C=O}}$). This establishes the nature of the reactive orbital for initiating the reaction to be $\pi\pi^*$ that is localized on the enamide functionality. Acyclic **1d** and **1e** are predicted to show the highest vertical excitation energies. This is in line with the observed reactivity with acyclic enamides. The vertical excitation energies of **1f** show that $\pi_{\text{enamide}} \rightarrow \pi^*$ and $n \rightarrow \pi^*$ transitions are close to each other (78.6 and 80.7 kcal/mol respectively), which indicates that both transitions are likely.

Mechanistically, under direct irradiation, the reactivity in **1f** originates from the $n\pi^*$ triplet excited state of the phenyl ketone chromophore. This implies that in **1f** the $n\pi^*$ excited state of carbonyl group initiates the reactions by interaction

with the ground-state alkene of the enamide leading to traditional Paternò–Büchi reaction. However, under sensitized irradiations, the carbonyl derivatives **1g–i** undergo reactions through a $\pi\pi^*$ triplet excited state that is localized on the enamide functionality leading to oxetane product. This unconventional oxetane product formation from an excited alkene that reacts with a ground state ketone (described as transposed Paternò–Büchi reaction) is advantageous to avoid the known side reactions of carbonyl excited states. Furthermore, utilizing one excited state to access two different products (cyclobutane and oxetane) is more appealing in terms of synthetic design and implementation as the orbital interactions initiating the reactions are different.^{16a,19} We are currently investigating this new approach of reversal of reactivity in similar systems to access novel chirally enriched oxetane building blocks.

CONCLUSIONS

Atropisomeric enamides were designed, and atropselective photocycloaddition reactions leading to chirally enriched cyclobutane and oxetane were investigated. The racemization kinetics provided insights into the energy barrier of racemization and optimal substituent design for stable axial chirality around the N–C_{Aryl} chiral axis, which resulted in high enantio- and diastereomeric excess in the photoproducts. Furthermore, by engineering the side chain of the enamide, the nature of the excited state was fine-tuned to be either an $n\pi^*$ configuration or a $\pi\pi^*$ configuration. Utilizing an $n\pi^*$ triplet excited state of the tether (e.g., **1f**), a traditional Paternò–Büchi reaction was observed under direct irradiation. By simply changing the irradiation to sensitized conditions, the reactivity was switched from $n\pi^*$ to $\pi\pi^*$ triplet excited state leading to a transposed Paternò–Büchi reaction. Such design allowed us to take advantage of $\pi\pi^*$ excited-state reactivity of enamide to yield both enantioenriched cyclobutanes (with ground state alkene tether as in **1a**) and oxetane (with a ground state carbonyl tether as in **1g–1i**) building blocks. Thus, our study has uncovered a unique method to target a specific excited state in a reacting chromophore by appropriate design modifications and by choosing appropriate irradiation conditions. This observation is expected to have a significant implication on the nature of the orbitals that initiates the photochemical transformations. Such investigations are currently underway in our laboratories.

COMPUTATIONAL METHODS

All calculations were performed using the Gaussian09 suite of quantum chemical program.²⁰ We have employed the long-range corrected Coulomb-attenuated method (CAM) in conjunction with the B3LYP functional for the present investigation.²¹ Pople's 6-31+G* basis set was used for all atoms.²² Solvent effects (acetone) were incorporated using the polarizable continuum model (PCM)²³ in its corrected linear response (cLR)²⁴ version for the excited states. Ground-state geometries were first optimized at the CAM-B3LYP/6-31+G* functional in conjunction with Pople's 6-31+G* basis set. All geometries were characterized as minima by Hessian calculations. Next, TD-DFT calculations were performed using the ground-state geometry at the CAM-B3LYP/6-31+G* level of theory to determine the vertical excitation energies. The nature of the excited state was determined by analyzing the coefficient of contributing transitions and through the visual inspection of the participating molecular orbitals in each of the transitions.

ASSOCIATED CONTENT

Supporting Information

The Supporting Information is available free of charge on the ACS Publications website at DOI: 10.1021/jacs.6b05936.

Single-crystal XRD data (CIF)

Experimental procedures, characterization data, analytical conditions, computational details and photophysical studies (PDF)

AUTHOR INFORMATION

Corresponding Authors

*E-mail: sj67@columbia.edu.

*E-mail: sunoj@chem.iitb.ac.in.

*E-mail: jayaraman.sivaguru@ndsu.edu.

ORCID

Elango Kumarasamy: 0000-0002-7995-6894

Raghavan B Sunoj: 0000-0002-6484-2878

J. Sivaguru: 0000-0002-0446-6903

Notes

The authors declare no competing financial interest.

ACKNOWLEDGMENTS

The authors from NDSU thank NSF for generous support (CHE-1213880 and CHE-1465075) of their research. E.K. and J.S. thank the NSF ND-EPSCoR for a doctoral dissertation fellowship (EPS-0814442). R.R. and J.S. thank the NDSU for doctoral dissertation fellowships. We thank the NDSU Center for Computationally Assisted Science and Technology (CCAST) for providing computational resources through the U.S. Department of Energy Grant No. DE-SC0001717. We thank Dr. Angel Ugrinov for solving the XRD structures.

REFERENCES

- (1) (a) Smith, S. W. *Toxicol. Sci.* **2009**, *110*, 4–30. (b) Brooks, W. H.; Guida, W. C.; Daniel, K. G. *Curr. Top. Med. Chem.* **2011**, *11*, 760. (c) LaPlante, S. R.; Edwards, P. J.; Fader, L. D.; Jakalian, A.; Hucke, O. *ChemMedChem* **2011**, *6*, 505–513. (d) Sunjic, V.; Parnham, M. J. *Signposts to Chiral Drugs: Organic Synthesis in Action*; Springer: Basel, Switzerland, 2011. (e) Kagan, H. B.; Gopalaiah, K. *New J. Chem.* **2011**, *35*, 1933–1937.
- (2) (a) Maskill, K. G.; Knowles, J. P.; Elliott, L. D.; Alder, R. W.; Booker-Milburn, K. I. *Angew. Chem., Int. Ed.* **2013**, *52*, 1499–1502. (b) Bos, P. H.; Antalek, M. T.; Porco, J. A.; Stephenson, C. R. J. *J. Am. Chem. Soc.* **2013**, *135*, 17978–17982. (c) Poplata, S.; Tröster, A.; Zou, Y.-Q.; Bach, T. *Chem. Rev.* **2016**, *116*, 9748–9815. (d) Mukhina, O. A.; Kutateladze, A. G. *J. Am. Chem. Soc.* **2016**, *138*, 2110–2113. (e) Kumar, N. N. B.; Mukhina, O. A.; Kutateladze, A. G. *J. Am. Chem. Soc.* **2013**, *135*, 9608–9611.
- (3) (a) Inoue, Y. *Chem. Rev.* **1992**, *92*, 741–770. (b) Rau, H. *Chem. Rev.* **1983**, *83*, 535–547.
- (4) (a) Ramamurthy, V. *Photochemistry in Organized and Constrained Media*; Wiley-VCH: New York, 1991. (b) Sivaguru, J.; Natarajan, A.; Kaanumalle, L. S.; Shailaja, J.; Uppili, S.; Joy, A.; Ramamurthy, V. *Acc. Chem. Res.* **2003**, *36*, 509–521. (c) Inoue, Y. In *Chiral Photochemistry*; Inoue, Y., Ramamurthy, V., Eds.; Marcel Dekker: New York, 2004; Vol. 11, p 129–177. (d) Vallavoju, N.; Selvakumar, S.; Jockusch, S.; Sibi, M. P.; Sivaguru, J. *Angew. Chem.* **2014**, *126*, 5710–5714. (e) Vallavoju, N.; Sivaguru, J. *Chem. Soc. Rev.* **2014**, *43*, 4084–4101. (f) Garcia-Garibay, M. A. *Acc. Chem. Res.* **2003**, *36*, 491–498. (g) Pemberton, B. C.; Raghunathan, R.; Volla, S.; Sivaguru, J. *Chem. - Eur. J.* **2012**, *18*, 12178–12190. (h) Pemberton, B. C.; Kumarasamy, E.; Jockusch, S.; Srivastava, D. K.; Sivaguru, J. *Can. J. Chem.* **2011**, *89*, 310–316. (i) Raghunathan, R.; Jockusch, S.; Sibi, M. P.; Sivaguru, J. *J. Photochem. Photobiol., A* **2016**, *331*, 84–88. (j) Ramamurthy, V. Acc.

- Chem. Res.* **2015**, *48*, 2904–2917. (k) Brimiouille, R.; Lenhart, D.; Maturi, M. M.; Bach, T. *Angew. Chem., Int. Ed.* **2015**, *54*, 3872–3890. (l) Vallavoju, N.; Selvakumar, S.; Jockusch, S.; Prabhakaran, M. T.; Sibi, M. P.; Sivaguru, J. *Adv. Synth. Catal.* **2014**, *356*, 2763–2768. (m) Vallavoju, N.; Selvakumar, S.; Pemberton, B. C.; Jockusch, S.; Sibi, M. P.; Sivaguru, J. *Angew. Chem., Int. Ed.* **2016**, *55*, 5446–5451.
- (5) (a) Clayden, J. *Angew. Chem., Int. Ed. Engl.* **1997**, *36*, 949–951. (b) Bencivenni, G. *Synlett* **2015**, *26*, 1915–1922.
- (6) (a) Ayitou, A. J.-L.; Sivaguru, J. *J. Am. Chem. Soc.* **2009**, *131*, 5036–5037. (b) Ayitou, A. J. L.; Fukuhara, G.; Kumarasamy, E.; Inoue, Y.; Sivaguru, J. *Chem. - Eur. J.* **2013**, *19*, 4327–4334. (c) Ayitou, A. J.-L.; Clay, A.; Kumarasamy, E.; Jockusch, S.; Sivaguru, J. *Photochem. Photobiol. Sci.* **2014**, *13*, 141–144. (d) Clay, A.; Kumarasamy, E.; Ayitou, A. J. L.; Sivaguru, J. *Chem. Lett.* **2014**, *43*, 1816–1825. (e) Ayitou, A.; Pemberton, B. C.; Kumarasamy, E.; Vallavoju, N.; Sivaguru, J. *Chimia* **2011**, *65*, 202–209. (f) Kumarasamy, E.; Raghunathan, R.; Jockusch, S.; Ugrinov, A.; Sivaguru, J. *J. Am. Chem. Soc.* **2014**, *136*, 8729–8737. (g) Kumarasamy, E.; Jesuraj, J. L.; Omliid, J. N.; Ugrinov, A.; Sivaguru, J. *J. Am. Chem. Soc.* **2011**, *133*, 17106–17109. (h) Kumarasamy, E.; Sivaguru, J. *Chem. Commun.* **2013**, *49*, 4346–4348. (i) Ayitou, A. J.-L.; Jesuraj, J. L.; Barooah, N.; Ugrinov, A.; Sivaguru, J. *J. Am. Chem. Soc.* **2009**, *131*, 11314–11315. (j) Raghunathan, R.; Kumarasamy, E.; Iyer, A.; Ugrinov, A.; Sivaguru, J. *Chem. Commun.* **2013**, *49*, 8713–8715. (k) Kumarasamy, E.; Raghunathan, R.; Sibi, M. P.; Sivaguru, J. *Chem. Rev.* **2015**, *115*, 11239–11300. (l) Raghunathan, R.; Kumarasamy, E.; Jockusch, S.; Ugrinov, A.; Sivaguru, J. *Chem. Commun.* **2016**, *52*, 8305–8308. (m) Kumarasamy, E.; Ayitou, A. J.-L.; Vallavoju, N.; Raghunathan, R.; Iyer, A.; Clay, A.; Kandappa, S. K.; Sivaguru, J. *Acc. Chem. Res.* **2016**, *49*, 2713–2724.
- (7) (a) Yang, N. C.; Nussim, M.; Jorgenson, M. J.; Murov, S. *Tetrahedron Lett.* **1964**, *5*, 3657–3664. (b) Horspool, W., Song, P.-S., Eds. *CRC Handbook of Organic Photochemistry and Photobiology*; CRC Press: Boca Raton, FL, 1995. (c) Griesbeck, A. G.; Fiege, M.; Bondock, S.; Gudipati, M. S. *Org. Lett.* **2000**, *2*, 3623–3625. (d) D'Auria, M.; Racioppi, R. *Molecules* **2013**, *18*, 11384–11428. (e) Griesbeck, A. G.; Abe, M.; Bondock, S. *Acc. Chem. Res.* **2004**, *37*, 919–928. (f) Kutateladze, A. G. *J. Am. Chem. Soc.* **2001**, *123*, 9279–9282.
- (8) Turro, N. J.; Ramamurthy, V.; Scaiano, J. C. *Modern Molecular Photochemistry of Organic Molecules*; University Science Books: Sausalito, CA, 2010; p 629.
- (9) (a) Swenton, J. S. *J. Chem. Educ.* **1969**, *46*, 217. (b) Schneider, R. A.; Meinwald, J. *J. Am. Chem. Soc.* **1967**, *89*, 2023–2032. (c) Coyle, J. D.; Carless, H. A. *J. Chem. Soc. Rev.* **1972**, *1*, 465–480. (d) Cho, S.-S.; Park, B.-S. *Bull. Korean Chem. Soc.* **2004**, *25*, 42–44. (e) Turro, N. J.; Dalton, J. C.; Dawes, K.; Farrington, G.; Hautala, R.; Morton, D.; Niemczyk, M.; Schore, N. *Acc. Chem. Res.* **1972**, *5*, 92–101. (f) Schuster, D. I. *Pure Appl. Chem.* **1975**, *41*, 601–633. (g) Turro, N. J.; Farneth, W. E.; Devaquet, A. *J. Am. Chem. Soc.* **1976**, *98*, 7425–7427.
- (10) (a) Schreiber, S. L. *Science* **1985**, *227*, 857–863. (b) Bach, T. *Synthesis* **1998**, *1998*, 683.
- (11) (a) Bach, T.; Schröder, J.; Harms, K. *Tetrahedron Lett.* **1999**, *40*, 9003–9004. (b) Bach, T.; Bergmann, H.; Brummerhop, H.; Lewis, W.; Harms, K. *Chem. - Eur. J.* **2001**, *7*, 4512–4521. (c) Vogt, F.; Jödicke, K.; Schröder, J.; Bach, T. *Synthesis* **2009**, 4268–4273.
- (12) Refer to [Supporting Information](#).
- (13) During the deprotection, the oxy anion cyclizes on to the double bond of the enamide resulting in significant amount of etherification products (for R1 = H and Me). This is the sole product if HF was used as the deprotecting agent.
- (14) Hubert, J. C.; Wijnberg, J. B. P. A.; Speckamp, W. N. *Tetrahedron* **1975**, *31*, 1437–1441.
- (15) Iyer, A.; Jockusch, S.; Sivaguru, J. *J. Phys. Chem. A* **2014**, *118*, 10596–10602.
- (16) (a) Turro, N. J.; Ramamurthy, V.; Scaiano, J. C. *Modern Molecular Photochemistry of Organic Molecules*; University Science Books: Sausalito, CA, 2010. (b) Zhang, Q.; Kuwabara, H.; Potscavage, W. J.; Huang, S.; Hatae, Y.; Shibata, T.; Adachi, C. *J. Am. Chem. Soc.* **2014**, *136*, 18070–18081. (c) Du, B.; Fortini, D.; Harvey, P. D. *Inorg. Chem.* **2011**, *50*, 11493–11505. (d) Froehlich, P. M.; Morrison, H. A. *J. Phys. Chem.* **1972**, *76*, 3566–3570.
- (17) Yagci, Y.; Jockusch, S.; Turro, N. J. *Macromolecules* **2007**, *40*, 4481–4485.
- (18) Sriyathne, H. D. M.; Thenna-Hewa, K. R. S.; Scott, T.; Gudmundsdottir, A. D. *Aust. J. Chem.* **2015**, *68*, 1707–1714.
- (19) (a) Jensen, F. R.; Beck, B. H. *J. Am. Chem. Soc.* **1968**, *90*, 3251–3253. (b) Dauben, W. G.; Salem, L.; Turro, N. J. *Acc. Chem. Res.* **1975**, *8*, 41–54.
- (20) Frisch, M. J.; Trucks, G. W.; Schlegel, H. B.; Scuseria, G. E.; Robb, M. A.; Cheeseman, J. R.; Scalmani, G.; Barone, V.; Mennucci, B.; Petersson, G. A.; Nakatsuji, H.; Caricato, M.; Li, X.; Hratchian, H. P.; Izmaylov, A. F.; Bloino, J.; Zheng, G.; Sonnenberg, J. L.; Hada, M.; Ehara, M.; Toyota, K.; Fukuda, R.; Hasegawa, J.; Ishida, M.; Nakajima, T.; Honda, Y.; Kitao, O.; Nakai, H.; Vreven, T.; Montgomery, J. A., Jr.; Peralta, J. E.; Ogliaro, F.; Bearpark, M.; Heyd, J. J.; Brothers, E.; Kudin, K. N.; Staroverov, V. N.; Kobayashi, R.; Normand, J.; Raghavachari, K.; Rendell, A.; Burant, J. C.; Iyengar, S. S.; Tomasi, J.; Cossi, M.; Rega, N.; Millam, N. J.; Klene, M.; Knox, J. E.; Cross, J. B.; Bakken, V.; Adamo, C.; Jaramillo, J.; Gomperts, R.; Stratmann, R. E.; Yazyev, O.; Austin, A. J.; Cammi, R.; Pomelli, C.; Ochterski, J. W.; Martin, R. L.; Morokuma, K.; Zakrzewski, V. G.; Voth, G. A.; Salvador, P.; Dannenberg, J. J.; Dapprich, S.; Daniels, A. D.; Farkas, O.; Foresman, J. B.; Ortiz, J. V.; Cioslowski, J.; Fox, D. J. *Gaussian 09*, revision D.01; Gaussian, Inc.: Wallingford, CT, 2013.
- (21) Yanai, T.; Tew, D. P.; Handy, N. C. *Chem. Phys. Lett.* **2004**, *393*, 51–57.
- (22) (a) Hariharan, P. C.; Pople, J. A. *Theor. Chim. Acta.* **1973**, *28*, 213–222. (b) Rassolov, V. A.; Pople, J. A.; Ratner, M. A.; Windus, T. L. *J. Chem. Phys.* **1998**, *109*, 1223–1229.
- (23) Tomasi, J.; Mennucci, B.; Cammi, R. *Chem. Rev.* **2005**, *105*, 2999–3094.
- (24) Caricato, M.; Mennucci, B.; Tomasi, J.; Ingrosso, F.; Cammi, R.; Corni, S.; Scalmani, G. *J. Chem. Phys.* **2006**, *124*, 124520.